ORIGINAL ARTICLE-ARAŞTIRMA

THE JOURNAL OF NEUROBEHAVIORAL SCIENCES
NÖRODAVRANIŞ BİLİMLERİ DERGİSİ

JNBS 2018 Published by Üsküdar University / 2018 Üsküdar Üniversitesi tarafından yayımlanmaktadır www.jnbs.org

Year (Yıl) : 2018
Volume (Cilt) : 5
Issue Number (Sayı) : 1
Doi : 10.5455/JNBS.1521311225

Received/Geliş: 17.03.2018
Accepted/Kabul:03.04.2018

RADIATION ATTENUATION PROPERTIES OF HUMAN BRAIN REGIONS ACCORDING TO ELEMENTAL COMPOSITION IN RADIOLOGICAL ENERGY RANGE: A MONTE CARLO SIMULATION

ELEMENTEL YAPILARINA GÖRE RADYOLOJİK ENERJİ DEĞERLERİNDE İNSAN BEYNİNİN FARKLI BÖLGELERİNİN RADYASYON ZAYIFLATMA ÖZELLİKLERİ: MONTE CARLO SİMÜLASYONU

Huseyin Ozan Tekin[1,2*], Turker Tekin Erguzel[3], Mesut Karahan[4], Muhsin Konuk[5], Nevzat Tarhan[6]

Abstract

This study aimed to investigate the radiation attenuation properties of seven brain regions namely Frontal, Occipital, Parietal, Temporal cortexes, Hippocampus, Thalamus and Cerebellum in terms of their elemental compositions. Monte Carlo N-Particle Transport Code System-extended (MCNPX) version 2.6.0 (Los Alamos National Lab, USA) general purpose Monte Carlo code has been employed in order to calculate the mass attenuation coefficients of those aforementioned brain regions. A satisfactory agreement has been obtained on the mass attenuation coefficients (μ/ρ) calculated by MCNPX and XCOM for those brain regions under investigation. The results underlined that Cerebellum has the highest mass attenuation coefficients in terms of the radiological energy values. This can be explained by the elemental mass fraction value of Chlorine (Cl) in Cerebellum. It could be deduced that the intensity of diagnostic radiation can be more attenuated in Cerebellum than rest of the brain regions during the brain CT or brain PET examinations. The data from the present paper would be useful for the use of standard simulation geometry and mass attenuation coefficients for medical physics as well as the applications of radiation physics.

Keywords: brain, mass attenuation coefficients, monte carlo

Özet

Bu çalışma, yedi beyin bölgesi olan Frontal, Occipital, Parietal, Temporal korteksler ve Hipokampus, Thalamus, Cerebellum'da ki radyasyon zayıflama özelliklerinin bölgelerin elementel kompozisyonları açısından araştırılmasını amaçlamıştır. Genel amaçlı Monte Carlo kodu Monte Carlo N-Particle Transport Code System-extended (MCNPX) 2.6.0 sürümü (Los Alamos Ulusal Lab, ABD) , yukarıda bahsedilen beyin bölgelerinin kütle zayıflama katsayılarını hesaplamak için kullanılmıştır. MCNPX ve XCOM tarafından elde edilen ve bahsedilen beyin bölgeleri için hesaplanan kütle zayıflama katsayıları (μ/ρ) üzerinde iyi bir uyum elde edilmiştir. Sonuçlar, Cerebellum'un radyolojik enerji değerlerinde en yüksek kütle zayıflatma katsayılarına sahip olduğunun göstermiştir. Bu durum, Cerebellum'daki Klorun (Cl) elementel kütle fraksiyonu değeri ile açıklanabilir. Tanısal radyasyonun yoğunluğunun beyin BT veya beyin PET taramaları sırasında beyin bölgelerinin geri kalanından daha fazla Cerebellum'da azalacağu düşünülebilir. Bu makaleden elde edilen verilerden standart simülasyon geometrisi ve kütle zayıflama katsayıları medikal fizik ve radyasyon fiziği uygulamalarında yararlı olacaktır.

Anahtar Kelimeler: *beyin, kütle zayıflatma katsayıları, monte carlo*

[1]Üsküdar University, Vocational School of Health Services, Radiotherapy Department, Istanbul, Turkey 34672
[2]Üsküdar University, Medical Radiation Research Center (USMERA), Istanbul, Turkey
[3]Üsküdar University, Faculty of Engineering and Natural Sciences, Software Engineering, Istanbul, Turkey
[4]Üsküdar University, Faculty of Engineering and Natural Sciences, Department of Bioengineering, Istanbul, Turkey
[5]Üsküdar University, Faculty of Engineering and Natural Sciences, Department of Molecular Biology and Genetics, Istanbul, Turkey
[6]Üsküdar University, Faculty of Humanities and Social Sciences, Department of Psychology, Istanbul, Turkey
[*]Corresponding Author: Dr. Huseyin Ozan Tekin, Üsküdar University, Vocational School of Health Services, Radiotherapy Department, Istanbul, Turkey 34672, E-mail: huseyinozan.tekin@uskudar.edu.tr

1. Introduction

Nowadays, due to the increasing applications of radiation-biological structure interactions, among researchers, there has been great attention paid to the simulation methods. Practical investigation on living tissues is not possible all the time. Therefore numerical methods and simulation studies have a major role in the field of radiation physics and medical physics. Permanent improvements in medical physics exposure reduction with the help of investigation are found in the day-to-day treatment of various types of diseases using radiation. On the other hand, methods for special care are required for radiation application in medical treatments to avoid undue exposure to normal human organs other than cancer of patient. The term of medical imaging is a valuable way of collecting visual or numerical internal organ information for the analysis and treatment processes. The medical image formation fact is dependent upon radiation interaction with material environments of body parts. The elemental density differences have a significant role in the medical imaging process. The density differences between the tissues and organs directly affect the attenuation of the radiation. Thus, penetration of radiation determines the contrast differences in the image formation. The term of medical imaging is being used in positron emission tomography (PET), computed tomography (CT), Mammography etc. for scanning different body parts. The contrast formation of the medical image depends upon the relative radiation attenuation in the tissue or organ. For monochromatic photon beams, the intensity decreases as the photon beam propagate through the sample or human body organ according to the Lambert-Beer law [$I=I0 \exp(-\mu t)$], upon where I0 is the incident intensity, t is the path length, and μ is the sample's linear attenuation coefficient. This coefficient depends on the elemental or composition chemical of the sample and is larger for electron-dense materials. Therefore, materials such as metal, bone, and kidney stones have high image contrast against soft tissues (Chen et al., 2012). The attenuation coefficient is basic fundamental photon interaction property of a material or human organ to investigate effective atomic number, effective electron density and shielding properties (Singh & Badier, 2016). The attenuation coefficients of various types of biological structures (cancerous and normal tissues) (Singh et al., 2015; Mirji et al., 2016; Tomal et al., 2010), body organs (Taylor, 2012), tissue substitutes have been investigated by different researchers. On the other hand, x-ray based medical imaging methods of the brain play vital role in the diagnostic process. Computed Tomography (CT) examination associates a series of X-rays images obtained from different angles to create the cross-sectional images of the patient. Computed Tomography (CT) of the head uses special x-ray equipment to help assess head injuries, severe headaches, dizziness, and other symptoms of an aneurysm, bleeding, stroke, and brain tumors. As previously mentioned, each density difference in tissue or organ can show a significant contrast formation in the medical image. The human brain can be grouped into a number of anatomical regions. The elemental mass fractions and concentrations have been shown to be heterogeneous (Stedman et al., 1995). The radiation attenuation properties of the brain have been investigated in the literature using Monte Carlo method (Tekin et al., 2017; Ermis et al., 2016). The literature review showed that recent studies handled the brain structure as a mathematical phantom with a certain elemental mass fractions (Elaff, 2016; 2018). However, radiation attenuation properties of different brain regions are not found in the literature. This has strongly encouraged us to investigate the attenuation properties of different brain regions compare them with each other. This study aimed to investigate the radiation attenuation properties of Frontal, Occipital, Parietal, and Temporal cortexes, Hippocampus, Thalamus, and Cerebellum considering their elemental compositions, respectively.

2. Materials and Methods

The mathematical simulation methods such as numerical modeling and Monte Carlo simulations are one of the vital methods to determine the physical problems when the experimental conditions are limited or hard to reach. In the current investigation, Monte Carlo N-Particle Transport Code System-extended (MCNPX) version 2.6.0 (Los Alamos National Lab, USA) general purpose Monte Carlo code has been employed for the calculations of mass attenuation coefficients of seven aforementioned brain regions considering their elemental compositions. MCNPX can provide fully three-dimensional simulation and can utilize extended nuclear cross section libraries and uses physics models for particle types (Briesmeister, 2000). In the literature, different studies have been performed using MCNPX Monte Carlo code for investigation of radiation mass attenuation coefficients and various shielding parameters for different type of materials (Tekin et al., 2017a; Akkurt et al., 2015; Tekin et al., 2016a; Tekin et al., 2016b; Tekin et al., 2017b; Tekin et al., 2017c; Erguzel et al., 2018; Tekin et al., 2017d; Dong et al., 2017; Laksminrayna et al., 2017; Tekin et al., 2017e; Tekin et al., 2018). The numerical applications and mathematical modeling methods of the radiation interaction problems mostly depend upon material compositions. The input structure of MCNPX code has some important parts to define the primary details of the simulation study. Those are the definition of the problem geometry, the definition of the materials with their chemical composition and the definition of the radiation source structure, respectively. In an MCNPX input file, the geometry is founded by defining geometric cells. The cells are surrounded by one or more geometric surfaces. In the present investigation, square prism geometry was employed for the modeling of each brain region. Since attenuation properties of different brain region have been investigated, they have been considered as independent biological structures, separately. Their edge lengths of this square prism geometry are defined as 5 cm while the axial z-length is defined for each simulation in different sizes because it is the thickness of the brain region. The inside of modeled square prism has been considered as a cell in the input file. For each calculation, this cell is modeled as a different brain region with their elemental mass fraction which given in Table 1 (Stedman & Spyrou, 1995). To model a cell with a certain elemental mass fraction, it should be defined as Mn in the material card. The MCNPX material card block provides the material definition according to

JNBS 2018 Published by Üsküdar University / 2018 Üsküdar Üniversitesi tarafından yayımlanmaktadır www.jnbs.org

the format required by the radiation transport code Monte Carlo N-Particle eXtended (MCNPX). The form of the material card can be shown as;

Mm ZZZ0001 fraction1 ZZZ0002 fraction2 ZZZ0003 fraction3

In this encoding structure, the acronym of n is the arbitrary material number match with material number in cell card and ZZZ is the atomic number of each element forming the material. In addition, fraction is the elemental mass fraction of the ZZZ in compound. In the present investigation, we have defined seven different brain region with their elemental mass fractions. The MCNPX encoding of the material cards of the brain regions samples from 1 to 7 can be seen as given below, respectively.

M1 6000 0.666337 7000 0.078218 8000 0.199010 11000 0.014851 12000 0.014851 17000

*0.017822 $**Frontal cortex***

*M2 6000 0.657143 7000 0.101478 8000 0.192118 11000 0.011823 12000 0.015764 17000 0.021675 $**Occipital cortex***

*M3 6000 0.680320 7000 0.087912 8000 0.187812 11000 0.017982 12000 0.010989 17000 0.014985 $**Parietal cortex***

*M4 6000 0.664343 7000 0.082669 8000 0.207171 11000 0.016932 12000 0.010956 17000 0.017928 $**Temporal cortex***

*M5 6000 0.646414 7000 0.093625 8000 0.196215 11000 0.025896 12000 0.017928 17000 0.019920 $ **Hippocampus***

*M6 6000 0.668322 7000 0.081430 8000 0.196624 11000 0.019861 12000 0.017875 17000 0.015889$ **Thalamus***

*M7 6000 0.565097 7000 0.115420 8000 0.200369 11000 0.013850 12000 0.083102 17000 0.022161 $ **Cerebellum***

As given above, M1 is the definition of material number and 6000 is the coding of the atomic number of Carbon since the atomic number of Carbon is 6. Finally, the value of 0.666337 is the elemental mass fraction of Carbon in the Frontal cortex. The rest of the M1 encoding can be considered and handled in this way. The mass attenuation coefficients of different brain regions were measured in a narrow beam transmission geometry using a point isotropic source with the collimated and mono-energetic beam. The radiation energy value of the point isotropic source has been defined for the 100 keV, 110 keV, 120 keV, 130 keV and 140 keV photon energies for each calculation, respectively. In the present MCNPX simulation, to obtain the absorbed dose amount in the detection field, average flux tally (F4) was employed. This kind of tally mash calculates the sum of the average flux in the cell. The analysis of recent investigation was performed using the D00205ALLCP03 MCNPXDATA package is comprised of DLC-200/MCNPDATA cross-section libraries. This library typically extends ENDF/B-VI data from 20 MeV to 150 MeV. The initial quantity of gamma ray is set as 108 particles. The mass attenuation coefficient calculations were done by using Intel® Core™ i7 CPU 2.80 GHz computer hardware. Finally, the error rate has been observed less than 0.1% in the output file. The total simulation geometry of the present investigation for the mass attenuation coefficient calculations can be seen in Figure 1.

Figure 1. Total simulation geometry

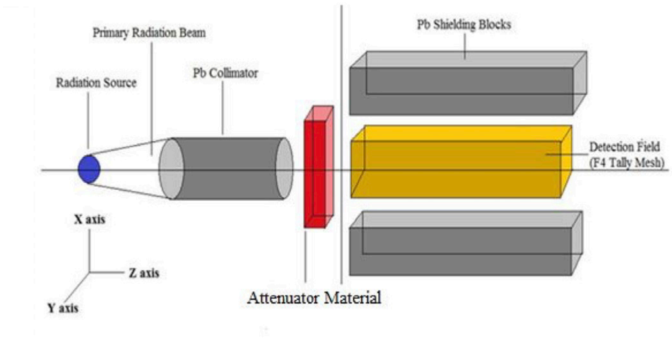

In addition, a cross-sectional screenshot of the MCNPX Monte Carlo code is given in figure 2.

Figure 2. Cross-sectional screenshot of MCNPX simulation geometry

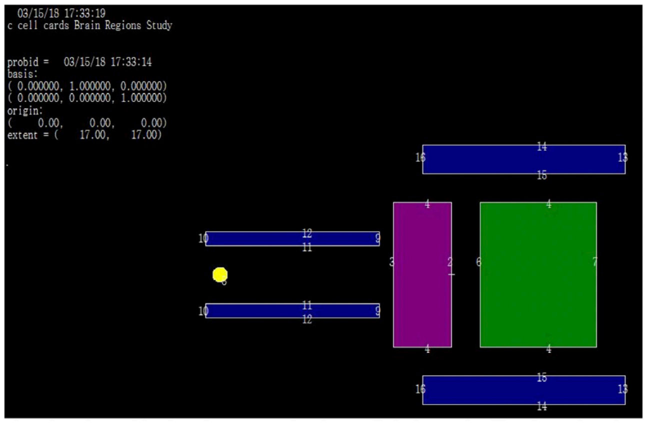

2.2. Mass attenuation coefficients

The mass attenuation coefficient (μ/ρ) of a brain region at a certain energy is the sum of the products of the weight fraction and the mass attenuation coefficient of the element i at that energy namely (Chantima & Kaewkhao, 2013).

$$\mu/\rho = \sum_{i} w_i(\mu/\rho)_i \qquad (1)$$

where wi and (μ/ρ)i are the fractional weight and the total mass attenuation coefficient of the ith constituent in the brain region. The mass attenuation coefficients of the elements constituting the brain region at certain energy were obtained from XCOM program (Berger et al., 1987).

3. Results and Discussions

The molecular formula of the different brain regions investigated in this study is presented in Table 1. The table also indicates the composition of each brain regions such as Frontal cortex, Occipital cortex, Parietal cortex, Temporal cortex, Hippocampus, Thalamus, and Cerebellum.

Table 1. The brain regions and their elemental mass fractions (%)

Brain Region	Carbon (C)	Nitrogen (N)	Oxygen (O)	Sodium (Na)	Magnesium (Mg)	Chlorine (Cl)
Frontal cortex	0.6663	0.0782	0.1990	0.0238	0.0149	0.0178
Occipital cortex	0.6571	0.1015	0.1921	0.0118	0.0158	0.0217
Parietal cortex	0.6803	0.0879	0.1878	0.0180	0.0110	0.0150
Tempo-ral cortex	0.6643	0.0827	0.2072	0.0169	0.0110	0.0179
Hip-pocam-pus	0.6464	0.0936	0.1962	0.0259	0.0179	0.0199
Thala-mus	0.6683	0.0814	0.1966	0.0199	0.0179	0.0159
Cerebel-lum	0.5651	0.1154	0.2004	0.0139	0.0831	0.0222

The mass attenuation coefficients (μ/ρ) for all brain regions have been calculated by MCNPX code for the 100 keV, 110 keV, 120 keV, 130 keV and 140 keV photon energies. Moreover, to prove the validity of the MCNPX results, we calculated the (μ/ρ) for the brain regions by XCOM program. The obtained results have been presented in Table 2.

Table 2. Mass attenuation coefficients of brain regions

Brain Region	100 keV		110 keV		120 keV		130 keV		140 keV	
	XCOM	MC-NPX	XCOM	MC-NPX	XCOM	MC-NPX	XCOM	MCNPX	XCOM	MCNPX
Frontal cortex	0.1536	0.1545	0.1491	0.1499	0.1451	0.1457	0.1415	0.1422	0.1383	0.1387
Occipital cortex	0.1538	0.1544	0.1492	0.1501	0.1452	0.1459	0.1416	0.1421	0.1383	0.1384
Parietal cortex	0.1533	0.1542	0.1489	0.1496	0.1449	0.1456	0.1414	0.1420	0.1382	0.1378
Temporal cortex	0.1535	0.1546	0.1490	0.1500	0.1451	0.1461	0.1415	0.1423	0.1383	0.1380
Hippocam-pus	0.1538	0.1550	0.1492	0.1506	0.1452	0.1462	0.1416	0.1425	0.1383	0.1382
Thalamus	0.1535	0.1547	0.1490	0.1498	0.1450	0.1456	0.1415	0.1423	0.1382	0.1384
Cerebellum	0.1550	0.1561	0.1501	0.1514	0.1459	0.1511	0.1421	0.1432	0.1388	0.1391
Correlation	0.9407		0.9433		0.9678		0.9410		0.7750	

The table also underlines the high correlation between the (μ/ρ) values calculated by MCNPX and XCOM for all brain regions under investigation. Aside from the tables given above, the investigation of the seven brain region response to the energy levels was worth focusing. As given in Fig 3 and Fig 4, it can be seen that the (μ/ρ) values were reduced exponentially with the increment of photon energy, and this indicates the increase of total interaction.

Figure 3. XCOM Mass Attenuation Coefficients for Various Radiation Energy Levels in Seven Brain Regions

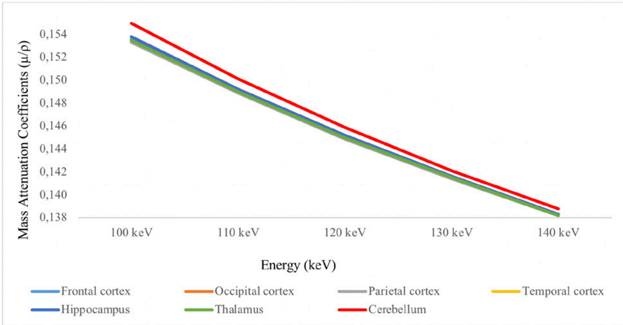

Figure 4. MCNPX Mass Attenuation Coefficients for Various Radiation Energy Levels in Seven Brain Regions

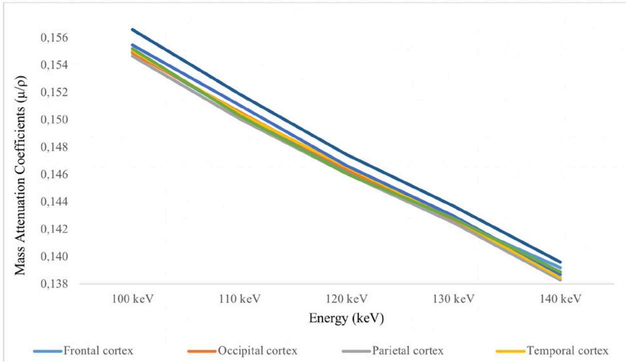

This behavior in (μ/ρ) was observed for all types of the brain regions. The small difference in the values of (μ/ρ) using MCNPX and XCOM establish the validity of the present MCNPX code. Furthermore, it is to be noted that, the attenuation behaviors of each brain regions observed similarly that is definitely due to similar elemental compositions of brain parts. However, Cerebellum has the highest mass attenuation coefficients in the studied radiological energy values. This can be explained by the elemental mass fraction value of Chlorine (Cl) in Cerebellum. Since the mass fraction of Chlorine is higher in Cerebellum, this behavior can be related to the effect of the atomic number on radiation attenuation. Therefore, Cerebellum might be expected to highest reducing the diagnostic X-rays energy, One can say that intensity of diagnostic radiation can be more attenuated in Cerebellum than in the rest of the brain regions during the brain CT or brain PET examinations.

4. Conclusion

It can be concluded that MCNPX code is one of the major and efficient codes for mass attenuation coefficients in low energy region and can be used for similar future studies where experimental conditions and data are not available. The data from the present paper would be useful for use of standard simulation geometry and mass attenuation coefficients for medical physics as well as the applications of radiation physics. It can be also concluded that calculated mass attenuation coefficients of different brain regions can be very useful for calculations of absorbed radiation dose values during the CT scans and other medical radiation studies.

References

Akkurt I, Tekin HO, Mesbahi A (2015) Calculation of detection efficiency for the gamma detector using MCNPX, Acta Phys. Pol. A. 128: 332–334. doi: 10.12693/APhysPolA.128.B-332

Berger, M.J., Hubbell, J.H., 1987. XCOM: photon cross sections database, web version 1.2,1999. Originally Published as NBSIR 87-3597 XCOM: Photon CrossSections on a Personal Computer, Washington, DC. Available from: http://physics.nist.gov/xcom.

Briesmeister, J., (2002). RSICC Computer Code Collection. MCNPX User's Manual Version 2.4.0. Monte Carlo N-Particle Transport Code System for Multiple and High Energy Applications, 2002.

Dong MG, El-Mallawany R, Sayyed MI, Tekin HO (2017). Shielding properties of 80TeO2--5TiO2--(15- x) WO3--xAnOm glasses using WinXCom and MCNP5 code. Radiat. Phys. Chem. 141:172–178. https://doi.org/10.1016/j.radphyschem.2017.07.006

Elaff, I., (2016). Brain tissue classification based on DTI: a comparative study between some clustering algorithms and their effect on different DTI scalar indices. Iranian Journal of Radiology 13(2):e23726. doi: 10.5812/iranjradiol.23726

Elaff, I., (2018). Comparative study between spatio-temporal models for brain tumor growth, Biochem Biophys Res Commun. 496(4):1263-1268. doi: 10.1016/j.bbrc.2018.01.183.

Erguzel, TT., Tekin, HO., Manici, T., Altunsoy, EE., (2018). Comparison of Multiple Linear Regression Analysis and Artificial Neural Network Approaches in the Estimation of Monte Carlo Mean Glandular Dose Calculations of Mammography. Digest Journal of nanomaterials and Biostructures.13(1).

Ermis, EE., Pilicer, FB., Pilicer, E., Celiktas, C., (2016). A comprehensive study of mass attenuation coefficients of different parts of the human body through Monte Carlo methods, Nuclear Science, and Techniques. 27:54. doi: 10.1007/s41365-016-0053-2

Hongyu, Chen., Melissa, M., Rogalski, Jeffrey., Anker, N., (2012). Advances in functional X-ray imaging techniques and contrast agents, Phys Chem Chem Phys. 14(39): 13469–13486

Lakshminarayana G, Baki SO, Kaky KM, Sayyed MI, Tekin HO, Lira A, Kityk IV, Mahdi MA (2017). Investigation of structural, thermal properties and shielding parameters for multicomponent borate glasses for gamma and neutron radiation shielding applications. J. Non. Cryst. Solids. 471:222-237. https://doi.org/10.1016/j.jnoncrysol.2017.06.001

Mirji, S., Badiger, NM., Kulkarni, SS., Tiwari, MK., (2016). Measurement of linear attenuation coefficients of normal and malignant breast tissues using synchrotron radiation, X-Ray Spectrometry, 45(3), DOI: 10.1002/xrs.2685.

N. Chanthima, J. Kaewkhao, (2013). Investigation on radiation shielding parameters of Bismuth borosilicate glass from 1 keV to 100 GeV, Ann. Nucl. Energy 55, 23–28.

Singh, VP. Badiger, NM., (2016). Photon interaction properties of some semiconductor detectors, Nuclear Reactor Technology, 27: 72. doi:10.1007/s41365-016-0076-8.

Singh, VP., Badiger, NM. (2013). Study of Effective Atomic Numbers and Electron Densities, Kerma of Alcohols: Phantom and Human Organ Tissue Substitutes, Nuclear Technology & Radiation Protection, Vol. 28 (2), pp 137-145.

Singh, VP., Badiger, NM., (2014). Effective atomic numbers of some tissue substitutes by different methods: a comparative study, Journal of Medical Physics,39(1), 24-31.

Singh, VP., Badiger, NM., (2015). Energy absorption buildup factors, effective atomic numbers and air-kerma for human body parts, vitamins and tissue substitutes, J. Radioanalytical and Nuclear Chemistry, 303 (3), 1983-1990.

Singh, VP., Badiger, NM., K., Nil, (2014). Assessment of methods for estimation of effective atomic numbers of common human organs and tissue substitutes: waxes, plastics, and polymers, Journal of Radioprotection, 49 (2), 115-121.

Stedman, JD., Spyrou, NM., (1995). Nutrition Supplement, 2, 542.

Taylor, ML., (2012). Quantification of differences in the effective atomic numbers of healthy and cancerous tissues: a discussion in the context of diagnostics and dosimetry, Med Phys. 39(9):5437-45

Tekin HO, (2016). MCNP-X Monte Carlo Code Application for Mass Attenuation Coefficients of Concrete at Different Energies by Modeling 3x3 Inch NaI (Tl) Detector and Comparison with XCOM and Monte Carlo Data, Sci. Technol. Nucl. http://dx.doi.org/10.1155/2016/6547318

Tekin HO, Manici T (2017) Simulations of mass attenuation coefficients for shielding materials using the MCNP-X code. Nucl. Sci. Tech. 28: 95. https://doi.org/10.1007/s41365-017-0253-4

Tekin HO, Manici T, Singh VP (2016) An Investigation on Shielding Effect of Bismuth on Lung Ct Scan Using Monte Carlo Simulation. Politek. Derg. 19: 617-622. doi:10.2339/2016.19.4

Tekin HO, Sayyed MI, Altunsoy EE, Manici T (2017) Shielding properties and effects of WO3 and PbO on mass attenuation coefficients by using MCNPX code. Dig. J. Nanomater. Biostruct. 12(3):861–867.

Tekin HO, Sayyed MI, Manici T, Altunsoy EE (2018). Photon shielding characterizations of bismuth modified borate - silicate-tellurite glasses using MCNPX Monte Carlo code. Materials Chemistry and Physics. 211: 9-16 doi: https://doi.org/10.1016/j.matchemphys.2018.02.009

Tekin HO, Singh VP, Kara Ü, Manici T, Altunsoy EE (2016) Investigation of nanoparticle effect on radiation shielding property using Monte Carlo method, Celal Bayar Univ. J. Sci. 12:195-199. http://dx.doi.org/10.18466/cbujos.92713

Tekin HO, Singh VP, Manici T (2017) Effects of micro-sized and nano-sized WO3 on mass attenuation coefficients of concrete by using MCNPX code. Appl. Radiat. Isot. 121:122–125. https://doi.org/10.1016/j.apradiso.2016.12.040

Tekin HO, Singh VP, Manici T, Altunsoy EE (2017). Validation of MCNPX with Experimental Results of Mass Attenuation Coefficients for Cement, Gypsum, and Mixture. J. Radiat. Prot. Res. 42:154–157. https://doi.org/10.14407/jrpr.2017.42.3.154

Tekin HO., Singh VP., Altunsoy EE., Manici T., Sayyed MI., (2017). Mass Attenuation Coefficients of Human Body Organs using MCNPX Monte Carlo Code. Iranian Journal of Medical Physics.

doi: 10.22038/ijmp.2017.23478.1230

Tomal, A., Mazarro, I., Kakuno EM., et al., (2010). Experimental determination of linear attenuation coefficient of normal, benign and malignant breast tissues. Radiat. Meas. 45, 1055–1059. doi:10.1016/j.radmeas.2010.08.008